

RESEARCH ARTICLE

A genome-scale *in vivo* RNAi analysis of epithelial development in *Drosophila* identifies new proliferation domains outside of the stem cell niche

Nicola Berns, Innokenty Woichansky, Steffen Friedrichsen, Nadine Kraft and Veit Riechmann*

ABSTRACT

The *Drosophila* oogenesis system provides an excellent model to study the development of epithelial tissues. Here, we report the first genome-scale *in vivo* RNA interference (RNAi) screen for genes controlling epithelial development. By directly analysing cell and tissue architecture we identified 1125 genes, which we assigned to seven different functions in epithelial formation and homeostasis. We validated the significance of our screen by generating mutants for *Vps60*, a component of the endosomal sorting complexes required for transport (ESCRT) machinery. This analysis provided new insights into spatiotemporal control of cell proliferation in the follicular epithelium. Previous studies have identified signals controlling divisions in the follicle stem cell niche. However, 99% of cell divisions occur outside of the niche and it is unclear how these divisions are controlled. Our data distinguish two new domains outside of the stem cell niche where there are differing controls on proliferation. One domain abuts the niche and is characterised by ESCRT, Notch and JAK/STAT-mediated control of proliferation. Adjacent to this domain, another domain is defined by loss of the impact of ESCRT on cell division. Thus, during development epithelial cells pass through a variety of microenvironments that exert different modes of proliferation control. The switch between these modes might reflect a decrease in the ‘stemness’ of epithelial cells over time.

KEY WORDS: *Drosophila* oogenesis, *In vivo* RNAi, Vps60, ESCRT, Notch, Epithelial development

INTRODUCTION

Epithelia form closely packed cell sheets covering the outside of the animal body and lining organs and cavities. Although epithelial tissues are central for development and homeostasis of all animals, very little is known about the genetic network underlying their formation. The follicular epithelium of the *Drosophila* ovary is a superb model to study the development of an epithelium. Like many vertebrate epithelia, the follicular epithelium originates from migrating mesenchymal precursor cells, which form a new epithelium in a process called mesenchymal epithelial transition (MET; Tepass et al., 2001). During MET the architecture of

mesenchymal cells is completely reorganised as reflected by the formation of adherens junctions, establishment of apical-basal membrane domains and repolarisation of the cytoskeleton.

The fly ovary is composed of 16–20 ovarioles consisting of a series of progressively older follicles, which are also called egg chambers. The egg chambers within an ovariole reflect the different stages of oogenesis, and allow investigators to follow the whole spectrum of epithelial development in a spatially ordered sequence (Horne-Badovinac and Bilder, 2005). Ovarioles originate in a structure called germarium, where egg chambers are assembled (Fig. 1, left part). At the anterior tip of the germarium, germline stem cells reside. They divide four times giving rise to a 16-cell germline cyst consisting of one oocyte and 15 supporting nurse cells. The cyst is initially covered by escort cells, which are released when the posteriorly moving cyst reaches the middle region of the germarium (region 2a and 2b). Here, the cysts encounter two follicle stem cell niches, and it has been proposed that cyst contact induces stem cell division (Nystul and Spradling, 2010). These divisions produce, in an alternating manner, follicle precursors migrating either laterally or in a posterior direction (Nystul and Spradling, 2007). Follicle cells continue to divide to generate ~30 epithelial cells, which are sufficient for the formation of an epithelial monolayer covering the cyst when it exits the germarium (Nystul and Spradling, 2010). Although it has been shown that Hedgehog, Wnt, BMP and JAK/STAT signalling pathways control division in the follicle stem cell niche (Forbes et al., 1996; Zhang and Kalderon, 2000; Zhang and Kalderon, 2001; Song and Xie, 2003; Kirilly et al., 2005; Vied et al., 2012), it is unclear how follicle cell proliferation is controlled outside of the niche.

Newly formed egg chambers exit the germarium in a process called ‘budding’. Individual egg chambers are connected by six to eight cells that form a ‘stalk’. The specification of stalk cells starts in the germarium at the border between region 2b and 3 (Nystul and Spradling, 2010; Chang et al., 2013). This process involves at least two signalling events. First, expression of Delta in the germline leads to activation of the Notch (N) pathway in the anterior follicle cells of a budding egg chamber (dark green cells in Fig. 1). Notch signalling induces ‘polar cell’ fate in these follicle cells (Ruohola et al., 1991; Grammont and Irvine, 2001; López-Schier and St Johnston, 2001). The polar cells then secrete Unpaired, which specifies stalk fate in further anterior-located follicle cells by activating the JAK/STAT pathway (Baksa et al., 2002; McGregor et al., 2002; Torres et al., 2003; Xi et al., 2003; Assa-Kunik et al., 2007). After budding the stalk is initially formed by two rows of wedge-shaped cells, which subsequently intercalate to form a single row of disc-shaped cells.

After exit from the germarium, the egg chamber grows rapidly and its development is subdivided into 14 stages (Spradling,

Heidelberg University, Medical Faculty Mannheim, Department of Cell and Molecular Biology and German Cancer Research Center (DKFZ), Division of Signaling and Functional Genomics, Ludolf-Krehl-Strasse 13-17, D-68167 Mannheim, Germany.

*Author for correspondence (veit.riechmann@medma.uni-heidelberg.de)

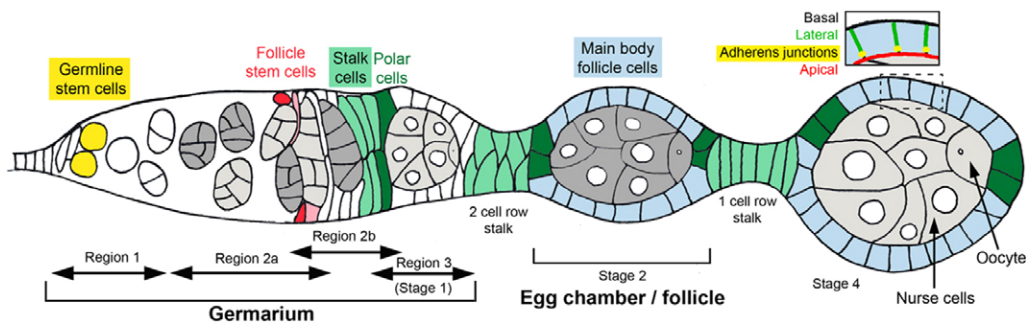


Fig. 1. Scheme showing a germarium and two egg chambers. Anterior is to the left in this and all subsequent figures. Germline stem cells (yellow) reside at the anterior tip of the germarium. Four divisions in region 1 of the germarium give rise to a 16-cell cyst (light and dark grey). Cysts move in posterior direction and contact follicle stem cells in region 2a and 2b (red), whose division generates stem cell daughters (pink). At the border between region 2b and 3 follicle cells in between two cysts are specified as polar (dark green) and stalk cells (light green). The remaining somatic cells become 'main body follicle' cells (blue). The germline cyst is shown in grey. In the inset (upper right corner) the apical membrane is depicted in red, the lateral membrane in green and the adherens junctions in yellow.

1993). A crucial aspect for epithelial development is the growth of the inner germline cysts. Cyst growth is compensated for by epithelial cell divisions, which enlarge the epithelial monolayer. It has been shown that cyst growth is induced by neural-derived insulin-like peptides (LaFever and Drummond-Barbosa, 2005), but it is unknown how proliferation in the epithelium is controlled. Cell divisions cease after stage 6 of oogenesis in a process mediated by activation of Notch signalling in epithelial cells, which is again induced by Delta expression in the germline (Deng et al., 2001; López-Schier and St Johnston, 2001; Poulton et al., 2011). Subsequently, epithelial morphogenesis starts with the formation of a squamous anterior and a columnar posterior epithelium.

Before morphogenesis occurs, all epithelial cells have a cuboidal shape. This cell shape is established during budding and is maintained until stage 7. Formation and maintenance of the cuboidal monolayer is dependent on apico-basal polarity. The apical membrane domain of the epithelium is facing the germline cyst, and their basal membrane domain opposes a muscle layer surrounding the ovary. Polarity is established in region 2b and 3 of the germarium, as revealed by formation of adherens junctions and apical accumulation of atypical protein kinase C (aPKC) (Franz and Riechmann, 2010). Loss of genes controlling polarity result in aberrant shapes and multilayering of epithelial cells. Moreover, some polarity genes like *lethal (2) giant larvae [Igl]*, also known as *Ig(2)I* act as tumour suppressors by restricting epithelial proliferation. Interestingly, loss of these genes also causes invasion of epithelial cells into the germline cyst (for a review, see Bilder, 2004).

To identify genes controlling epithelial formation, polarisation and proliferation, we performed an *in vivo* RNA interference (RNAi) screen in the follicular epithelium in a genome-scale approach. We induced gene expression knockdown specifically in the epithelium and assessed histological defects at the tissue and cell level directly by dissecting and staining ovaries in a high-throughput procedure. We distinguished seven different phenotypic categories according to the developmental phase when they occur and according to the identified histological defects. We screened half of the *Drosophila* genome and identified functions for 1125 genes in epithelial development.

To show that our screen identifies new genes whose characterisation sheds light on the mechanisms regulating epithelial development we further analysed the *Drosophila*

orthologue of *Vps60*, a component of the endosomal sorting complexes required for transport (ESCRT) machinery. In a proof of principle approach, we validated the *Vps60* RNAi phenotype by the generation of a loss-of-function mutation. Moreover, we show how *Vps60* and other members of the ESCRT machinery control epithelial organisation and proliferation specifically during the formation of the follicular epithelium. Our data indicate that the ESCRT machinery restricts epithelial proliferation by downregulating Notch and JAK/STAT activity. Importantly, this function is limited to the germarium, and thus marks the existence of a spatially restricted proliferation domain within the developing epithelium.

RESULTS

Screen design

To identify new genes controlling the development of the follicular epithelium we performed an *in vivo* RNAi screen. We randomly selected 7653 genes from the KK library (Vienna *Drosophila* RNAi Center, VDRC) for UAS/GAL4-mediated knockdown in the follicular epithelium (see Fig. 2 for the screening procedure). In a primary screen, we induced the UAS-RNAi constructs using a combination of GAL4 driver lines that are active in follicle stem cells (*escargot-GAL4*; Micchelli and Perrimon, 2006) and in epithelial cells (*GRI-GAL4*; Gupta and Schüpbach, 2003), resulting in an almost continuous gene knockdown during epithelial development. A total of 2084 (27%) of the RNAi lines caused lethality under these conditions. As we assumed that lethality was in most cases caused by *escargot-GAL4* activity during earlier stages of development we screened the lethal lines with the *GRI-GAL4* driver alone, which allowed us to identify 618 additional candidates. A total of 238 lines still caused lethality with *GRI-GAL4*. To screen these lines we used the driver line *traffic jam-GAL4* that was published during the course of our screen and which induces expression in all cells of the follicular epithelium including stem cells (Olivieri et al., 2010). Using this driver we identified 157 more candidates. In summary, we analysed 99% of the selected genes for a function in epithelial development and identified 1381 candidates in the primary screen.

Phenotypes were identified by analysing histological samples of knockdown epithelia, which we generated by applying a high-throughput staining method (Berns et al., 2012). We visualised the epithelium by staining nuclei with DAPI and the

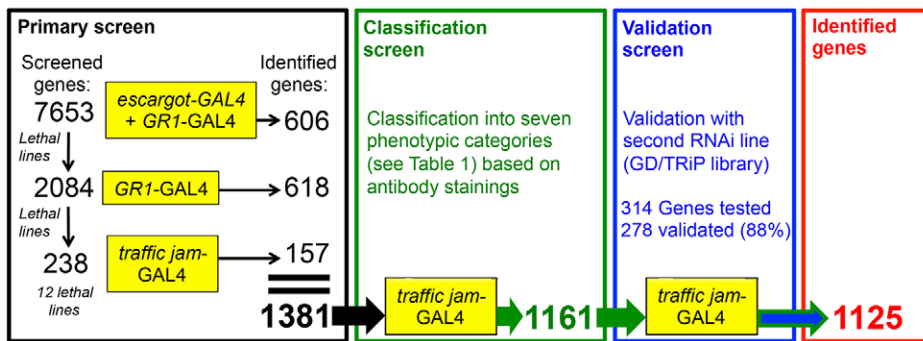


Fig. 2. Flowchart showing the different steps of the *in vivo* RNAi screen. See text for details.

epithelial cytoplasm by co-expressing UAS-GFP. This allowed a preliminary distinction of genes affecting the formation of the epithelium and genes affecting later stages of epithelial development (see below).

We described the phenotypes of the identified candidates more precisely in a classification screen for which we performed stainings with antibodies highlighting the apical (aPKC) and lateral [Discs large (Dlg)] membrane domains of epithelial cells. Stainings were analysed with wide-field and confocal microscopes to detect defects affecting tissue and organ morphology and epithelial cell shape and polarity. For 147 genes, these defects were so strong that no ovaries could be dissected. The remaining genes were categorised into different phenotypic groups (see below). Complete lists of screened RNAi lines and of the identified genes with corresponding phenotypes are shown in supplementary material Table S1. The classification screen was carried out with *traffic jam-GAL4*. As we identified the vast majority of candidates in the primary screen with *escargot-GAL4* and *GRI-GAL4*, the use of *traffic jam-GAL4* allowed us to retest these lines with a different driver. Taken together, we confirmed a function in epithelial development for 1161 (84%) of the genes identified in the classification screen.

After screening the first 1000 lines, we selected 49 candidate genes for a validation test, for which we used RNAi lines from the GD library (VDRC, Dietzl et al., 2007) targeting a different sequence of the same gene. This first validation screen confirmed 48 (98%) of the candidates. After screening our complete set of genes, we chose 265 additional genes for a second validation test. Here, we neglected genes whose functions are thought not to be specific to epithelial cells (e.g. ribosomal proteins) and selected genes for which fly stocks from the newly generated TRiP library (Harvard Medical School) were available. In this screen 230 genes (87%) were positive. Collectively, we validated 88% of the genes in two validation screens indicating a low false-positive rate. After removal of genes that were not validated, we identified 1125 genes in total (Fig. 2). This indicates that ~15% of the analysed genes contribute to the development of the follicular epithelium.

Phenotypic categories in the formation phase

Phenotypes identified in the classification screen were subdivided according to the stage when they first appear. We distinguished an epithelial ‘formation phase’ in the germarium from a ‘maintenance phase’ (stage 2–6), during which the epithelial cells maintain their cuboidal shape.

In the formation phase, different cellular processes orchestrate the assembly of a monolayered epithelium. First, divisions in the stem cell niche and in other regions of the germarium produce

sufficient epithelial cells to encapsulate the germline cyst. Second, epithelial precursors separate individual cysts by migrating in between them. Third, mesenchymal precursors undergo MET to adopt an epithelial state, which involves the formation of adherens junctions, the establishment of apical, lateral and basal membrane domains, and polarisation of the cytoskeleton (Tanentzapf et al., 2000; Franz and Riechmann, 2010). This process also includes cell shape changes necessary to form a monolayer of cuboidal cells. If migration, MET or cell divisions are affected, epithelial development will be impaired in the formation phase.

We distinguished five different phenotypic categories within the formation phase. First, we detected ‘epithelial gaps’ in stage 1 and 2 follicles, indicating that epithelial formation had already been affected in the germarium (Fig. 3B; Table 1). To identify possible mechanisms mediating epithelial development, we analysed the frequency of gene ontology (GO) terms among the genes of a certain phenotypic category (see Materials and Methods). However, in the case of the epithelial gaps category we found no significant enrichment in any GO terms.

The second phenotypic category in the formation phase is found for genes whose knockdown abolishes cyst encapsulation and results in germline cysts completely lacking an epithelium. We named this phenotype ‘tube-like’ as the affected ovarioles look like tubes in which naked cysts pile up (Fig. 3D; supplementary material Fig. S1A). Prominent examples in this group are α - and β -Catenin and Cdc42. Cdc42 is a member of the protein complex establishing the apical membrane domain (Joberty et al., 2000; Lin et al., 2000; Qiu et al., 2000), and its knockdown leads to severe membrane polarity defects and rounded cell shapes (supplementary material Fig. S1B). This confirms a central role of this protein for cell polarity and epithelial formation. Similarly, knockdown of Catenins abolishes cyst encapsulation, which confirms earlier results (Sarpal et al., 2012). The Catenins knockdown phenotype can be explained with their crucial role in adherens junction assembly. Besides these genes involved in ‘cytoskeletal organisation’, GO term analysis in the tube-like group reveals an enrichment of genes involved in translation (e.g. ribosomal subunits). Their knockdown is unlikely to affect cell adhesion or polarity but appears to severely reduce the number of epithelial cells (Fig. 3D). We speculate that a strong reduction in protein synthesis prevents cell cycle progression of follicle cells in the germarium, which reduces their number to such an extent that cyst encapsulation is abolished.

The third phenotypic category does not result from a block but rather from impairment in the process of cyst separation and results in ‘compound egg chambers’. In contrast to wild-type egg

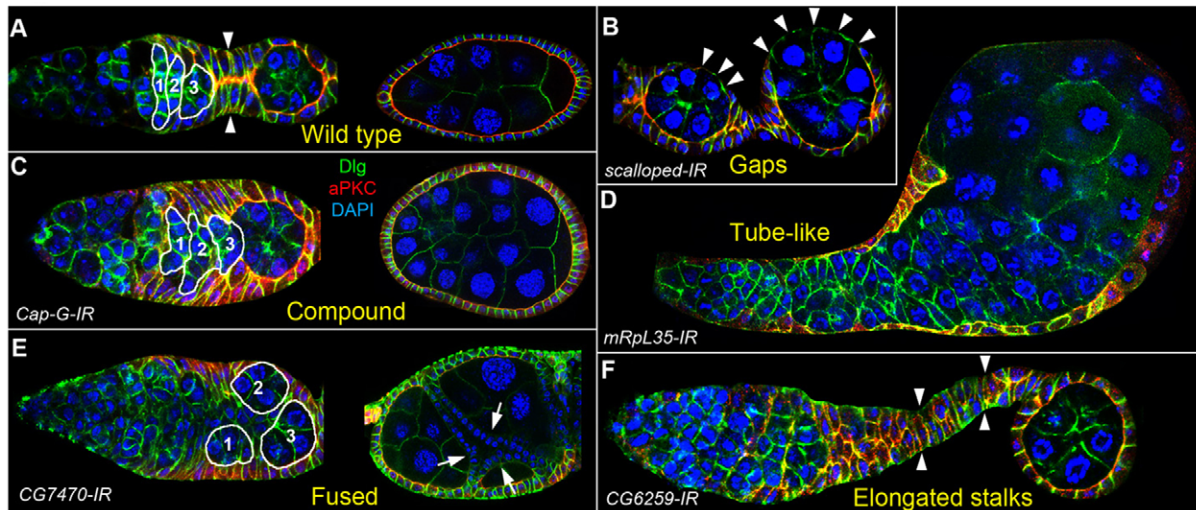


Fig. 3. Phenotypic categories in the formation phase. See Table 1 for schematic representations of phenotypes. (A) A wild-type germarium (left) and egg chamber (right) stained for aPKC (red), Dlg (green) and DAPI. Three progressively older germline cysts in the germarium are marked with white lines. The stalk is indicated with arrowheads. (B) Knockdown of *scalloped* leads to gaps (arrowheads) in the epithelium of young egg chambers. (C) Knockdown of the Condensin subunit Cap-G results in the formation of compound egg chambers as revealed by the presence of additional nurse cell nuclei (compare the number of cyst nuclei with A). Defects in cysts encapsulation are detectable in the germarium where cysts are not properly separated. (D) Knockdown of the mitochondrial ribosomal protein L35 (mRpl35) leads to the formation of tube-like ovarioles. Only a few follicle cells are detectable, indicating a reduction in cell number. (E) *CG7470* RNAi leads to the formation of fused egg chambers in which individual egg chambers are covered by an epithelium (arrows) but not separated by a stalk. (F) Knockdown of the *Drosophila* Vps60 orthologue *CG6259* results in the formation of elongated stalks (arrowheads).

chambers, which consist of one cyst, compound egg chambers comprise two or more cysts, which are not separated by epithelial cells (Fig. 3C, right). Compound egg chambers can be readily recognised at later stages of oogenesis by their increased number of nurse cell nuclei (e.g. 30 or 45 instead of 15). The compound group shows an enrichment of genes implicated in cell migration, which might reflect a function of the genes in regulating the migration of precursor cells in between the cysts. Moreover, we find that genes implicated in translation and mRNA processing are highly enriched in this group. mRNA processing defects might, like translation defects, lead to reduced protein synthesis and inhibit cell cycle progression. A decrease in epithelial cell numbers might be compensated for by encapsulating more than one cyst into one epithelial layer. Consistent with the idea that decreased cell numbers lead to compound follicles, we found that genes involved in the cell cycle process and spindle organisation (e.g. *pebble*) are also overrepresented.

The fourth phenotypic category is when the formation of the stalk connecting the epithelium of individual egg chambers is affected. In the absence of a stalk, each cyst is completely encapsulated by one epithelial layer, but neighbouring follicles are closely linked with each other, resulting in the formation of ‘fused’ egg chambers (Fig. 3E, right). Specification of stalk cell fate is mediated by JAK/STAT signalling and, consistent with this, we identified members of this pathway in the fused category. Moreover, proper stalk formation is dependent on shape changes and rearrangements of specified precursor cells. These processes are reflected by an enrichment of genes involved in ‘anatomical structure morphogenesis’.

Stalk cells are recruited in the germarium from cells that lie between cysts (Fig. 1, light green cells). Stalk formation is therefore (like cyst separation) dependent on the migration of precursors between the cysts. Likewise, cyst separation and stalk formation are both dependent on sufficient epithelial cells, and therefore sensitive to a reduction in cell number. Consistent with

this, we also found GO term enrichment of ‘cell migration’ and ‘cell cycle’ in the fused category. The close relationship between the fused and compound categories is further supported by the fact that 65% of the genes that cause fused egg chambers also lead to compound follicles (see also supplementary material Table S3).

The fifth phenotypic category was ‘elongated stalks’. This occurred upon knockdown of genes that are required to restrict the number of cells forming the stalk. A stalk is normally formed by six to eight cells, and we identified several genes whose knockdown resulted in an increase in the number of cells connecting the two follicles (Fig. 3F). Genes in this group and the mechanisms leading to the formation of elongated stalks are discussed below.

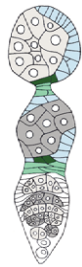
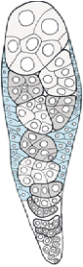
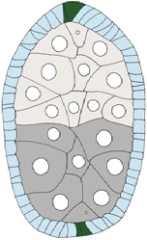
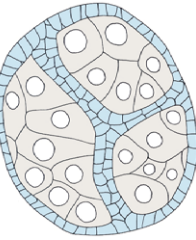

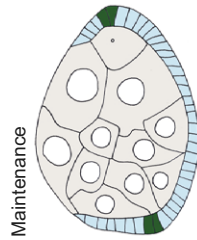
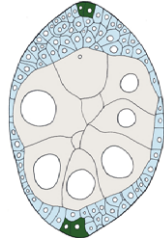
Phenotypic categories in the maintenance phase

After budding from the germarium newly formed egg chambers start to grow. This growth is dependent on an insulin-triggered volume increase of the inner germline cyst (LaFever and Drummond-Barbosa, 2005), which generates a tensile force that acts on the epithelial layer. It has been shown that loss of cell adhesion or actomyosin contractility leads to flattening of epithelial cells indicating that the epithelium resists a physical stress, which strains the cytoskeleton and adhesive forces between cells (Müller, 2000; Tanentzapf et al., 2000; Wang and Riechmann, 2007). This tensile stress is relieved by epithelial cell divisions, which result in an enlargement of the epithelial surface. We refer to this period between stage 2 and 6 as the ‘maintenance phase’, within which we identified two major phenotypic categories: ‘epithelial ruptures’ and ‘multilayering’.

Epithelial ruptures

Epithelial ruptures are characterised by holes in the epithelium that, in contrast to epithelial gaps, are detectable only after stage

Table 1. Phenotypic categories identified in the screen

Developmental phase	Phenotypic category	Description	GO term enrichment (cellular process)	Examples	
Formation	 Epithelial gaps (<i>n</i> =341)	Incomplete epithelial monolayer at stage 2.	No term enrichment	<i>rigor mortis</i>	
		 Tube-like ovaries (<i>n</i> =130)	Cyst encapsulation abolished.	Translation; cytoskeleton organisation	α -Catenin; <i>Cdc42</i> ; ribosomal subunits
	 Compound egg chambers (<i>n</i> =417)	Cyst separation affected, more than one cyst encapsulated by one monolayer.	Translation; mRNA processing; spindle and cytoskeleton organisation; cell cycle process; cell migration	<i>pebble</i>	
		 Fused egg chambers (<i>n</i> =114)	Stalk formation affected, cysts with complete monolayers are not separated by a stalk.	Cell migration; anatomical structure; morphogenesis; cell cycle; cytoskeleton organisation; JAK/STAT cascade	<i>domeless</i>
	Maintenance	 Elongated stalks (<i>n</i> =32)	Increased numbers of cells between two adjacent egg chambers.	Endosomal transport; cell morphogenesis; actin nucleation; cell polarity	<i>Vps60</i>
		 Epithelial ruptures (<i>n</i> =386)	Parts of the cyst are not covered by epithelial cells (occurs after stage 2).	mRNA processing; translation; mitotic spindle organisation; cell cycle	<i>kon-tiki</i> ; <i>fascetto</i>
 Epithelial multilayering (<i>n</i> =104)	Monolayer transformed into double- or multi-layer. Affects either locally restricted areas or the whole epithelium. Few genes also cause invasiveness into germline cysts.	Morphogenesis; cell proliferation; adherens junction organisation; cell polarity; vesicle transport	<i>par-6</i> ; α -Spectrin		

The schematics show typical examples of the different phenotypic categories. See Fig. 1 for a wild-type reference. Follicle cells are depicted in blue, stalk cells in light green, polar cells in dark green and germline cysts in grey. *n*, the number of genes identified in each phenotypic category. Enriched GO terms listed are selected according to their significance for epithelial development (see also Materials and Methods). See supplementary material Table S2 for a complete list of enriched GO terms.

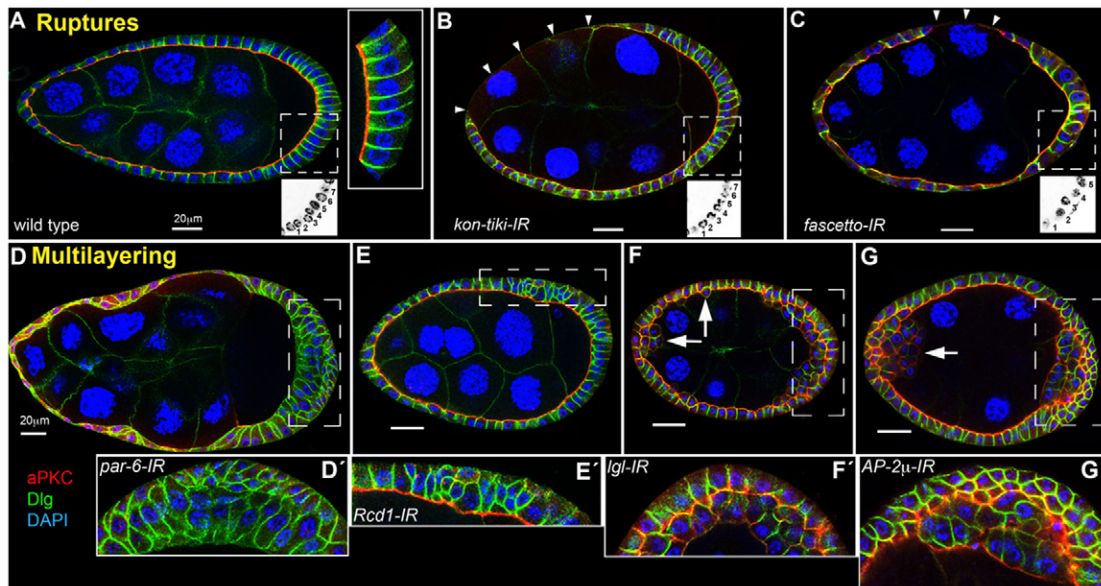


Fig. 4. Phenotypic categories in the maintenance phase. (A–C) Epithelial ruptures. (A) Wild-type egg chamber. (B) Knockdown of *kon-tiki* and (C) *fascetto* result in rupture of the epithelium (arrowheads). Lower insets show the DAPI channel of the region indicated by the dashed box. Seven nuclei are detectable in the wild type and after *kon-tiki* RNAi. After *fascetto* RNAi, only five cells are detectable. The upper inset in A shows cells marked by the dashed box at a higher magnification. (D–G) Epithelial multilayering. (D) *par-6* RNAi affects the architecture of the whole epithelium. (D') Four to five rows of epithelial cells with aberrant shapes. The loss of the apical marker aPKC reflects the function of *par-6* in establishing the apical membrane domain. (E) Knockdown of *Reduction in Cnn dots 1 (Rcd1)* leads to multilayering in a locally restricted region of the epithelium (shown in E'). Cells in the multilayer lose aPKC and round up. (F,G) Knockdown of *lgl* (F) and *AP-2μ* (G) cause multilayering especially at the anterior and posterior poles of the egg chamber. Cells in the multilayer lose their shape (F',G'). Some cells in the multilayer ingress into the germline cyst (arrows).

2. Egg chambers with ruptures can be easily recognised by regions in which the cyst is not covered by epithelial cells (Fig. 4B,C, arrowheads). Analysis of GO terms reveals a strong enrichment of genes involved in ‘mRNA processing’, ‘translation’ as well as ‘mitotic spindle organisation’ and ‘cell cycle’. These genes are directly (spindle organisation and cell cycle) or might be indirectly (mRNA processing and translation) involved in cell cycle progression of epithelial cells. As epithelial proliferation is essential to accommodate the volume increase of the cyst, the epithelium tears apart when mitosis is blocked. Fig. 4C shows the phenotype of *fascetto*, a gene required for spindle formation and cytokinesis as an example for this group (Verni et al., 2004). Its knockdown led to reduced epithelial cell numbers and ruptures.

A comparison of co-occurrence of phenotypes (supplementary material Table S3) reveals that genes whose knockdown cause tube-like ovaries also frequently lead to ruptures (54%). Similarly, genes causing compound egg chambers frequently lead to ruptures (44%). As one important cause for all three phenotypes is a reduction of epithelial cells, we propose that a reduction in cell number has different consequences at different developmental stages. A reduction in cell proliferation during the formation phase leads, in strong cases, to tube-like ovarioles and, in weaker cases, to compound egg chambers. At later stages of oogenesis, reduced proliferation leads to rupture of the epithelial layer.

Although a reduction in cell number seems to be one major reason for the emergence of ruptures, epithelial integrity is also dependent on cell adhesion and the actin cytoskeleton. Therefore, genes controlling adhesion and cytoskeletal organisation are also included in this phenotypic group. Along this line, we found that knockdown of the Cadherin-domain-containing protein Kugelei

and of a subunit of the Arp complex (*Arpc1*) led to ruptures. Moreover, the rupture group contains genes which orchestrate adhesion and cytoskeletal organisation, like *kon-tiki* (Fig. 4B), which encodes a transmembrane protein required for interaction between myotubes and tendon cells during muscle development (Schnorrer et al., 2007).

Multilayered epithelia

The other phenotypic category in the maintenance phase is the transformation of a monolayered epithelium into two or even more cell layers (‘epithelial multilayering’, Fig. 4D–G). As expected we find an enrichment of genes involved in ‘morphogenesis’, ‘adherens junction organisation’ and ‘cell polarity’ in this category. Prominent examples are polarity regulators like *par-6* (Fig. 4D) and the actin cross-linker α -*Spectrin*, which are known to control cell polarity, cytoskeleton and morphogenesis.

Genes associated with the term ‘cell proliferation’ are also highly enriched in the multilayer group. Among them are negative cell cycle regulators, like the tumour suppressor gene *lgl* whose knockdown leads to overproliferation (Fig. 4F). Multilayering in such cases can be explained by the fact that more epithelial cells are produced than required for a monolayered epithelium. Defective tissue architecture is further promoted by additional functions of tumour suppressor genes in controlling cell polarity. Another distinctive group in the multilayer category are genes involved in ‘vesicle transport’ (e.g. *Rab5* and *Shibire/Dynamain*), confirming previous studies which show that regulation of endocytosis is central for epithelial integrity (Lu and Bilder, 2005; Georgiou et al., 2008; Harris and Tepass, 2008; Leibfried et al., 2008; Morrison et al., 2008).

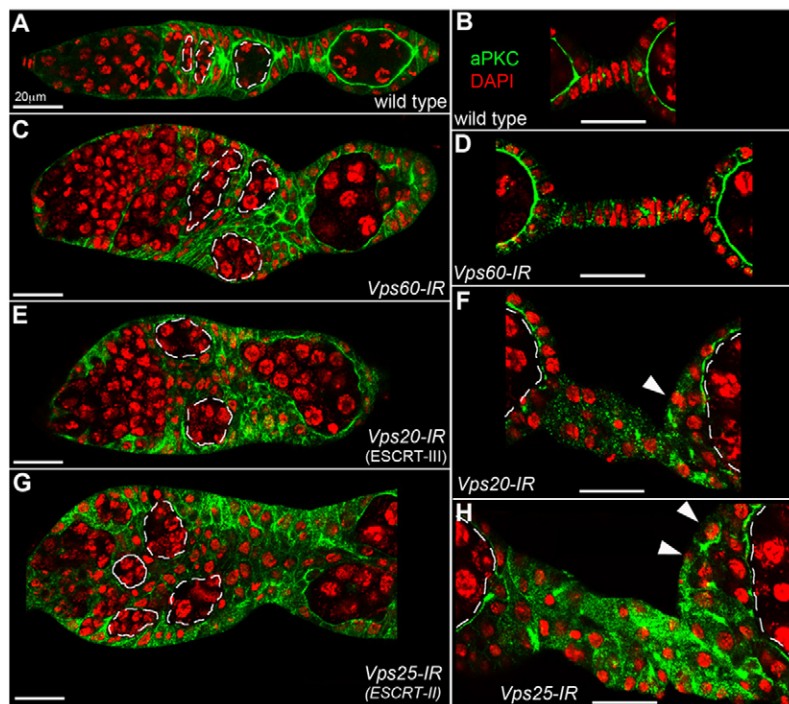


Fig. 5. The ESCRT machinery is required for germarial organisation and stalk length restriction. (A) Wild-type germarium showing aPKC (green) and nuclei (red). Three progressively older cysts are marked by the dashed line, highlighting their linear arrangement. (B) Wild-type stalk connecting two follicles outside of the germarium. *Vps60* RNAi disturbs the linear arrangement of cysts (C), and leads to the formation of an elongated stalk (D). Knockdown of *Vps20* (E) and *Vps25* (G) lead to the same defects in the germarium as seen for *Vps60*. *Vps20* (F) and *Vps25* (H) knockdowns also result in an increase of cells between two follicles. In contrast to *Vps60*, these cells show no ordered arrangement. Some cells accumulate at the poles of the egg chamber (arrowheads). The dashed white line in F and H marks the border of the cysts.

We further subdivided the group of genes whose knockdown resulted in the multilayer phenotype into genes affecting the whole tissue architecture (Fig. 4D,F,G) and genes affecting epithelial organisation only in locally restricted areas (Fig. 4E). Local defects were for instance observed after knockdown of genes encoding phosphoinositol-modifying enzymes. Global defects in epithelial organisation were detectable after knockdown of polarity genes and certain components regulating vesicle trafficking (*Rab5*, *Rab11* and *Syntaxin7/avalanche*).

Within the multilayering category we also identified phenotypes where individual cells or clusters of cells seem to

ingress into the germline cyst (arrows in Fig. 4F,G). In this subgroup, we found genes causing strong and highly penetrant phenotypes (supplementary material Table S1, marked with ‘S’) and genes that caused ‘invasive’ events with a weak penetrance (supplementary material Table S1, marked with ‘W’). Among the highly penetrant genes were *lgl*, which is known to cause invasiveness (Bilder et al., 2000) and *Adaptor protein 2 subunit μ* (*AP-2 μ*), for which this phenotype had not been previously described. The phenotype of the *AP-2 μ* knockdown closely resembled that of *lgl* knockdown and is reflected by a simultaneous loss of cuboidal cell shape and cell ingression

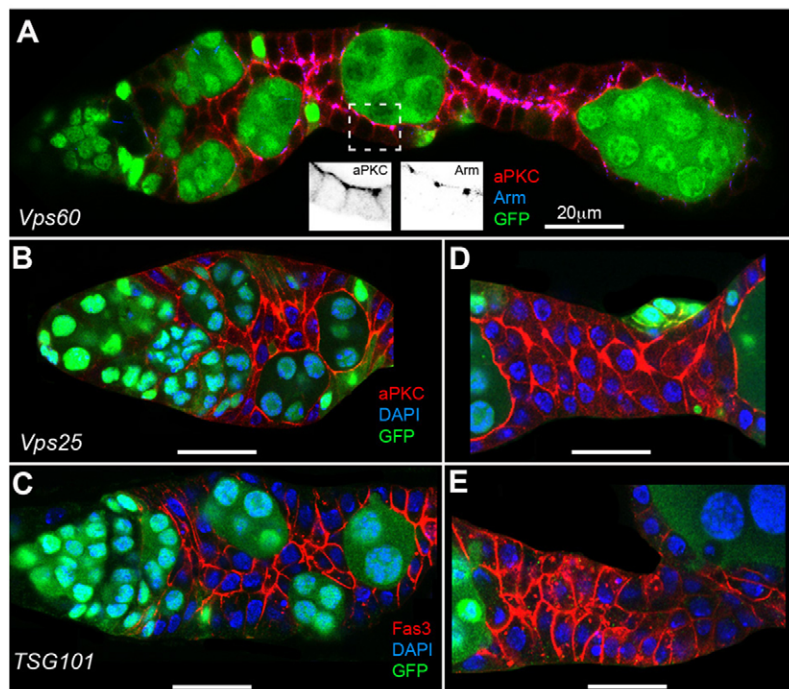


Fig. 6. Validation of RNAi-mediated ESCRT phenotypes. (A) Germarium consisting of *Vps60* mutant cells stained for aPKC (red) and the adherens junction marker Arm (blue). The germline cysts are wild type and stained in green. The linear alignment of cysts in the germarium is abolished and the stalk (right) is elongated. Insets show single channels of aPKC and Arm. Germaria with *Vps25* (B) and *tsg101* (C) mutant cell clones showing misalignment of germline cysts. *Vps25* (D) and *tsg101* (E) mutant cells connecting two egg chambers outside of the germarium. Cell numbers between two cysts are dramatically increased. Note that red staining of *Vps25* mutants reveals aPKC localisation, whereas *tsg101* mutants are stained for the lateral marker Fascin 3 (Fas3).

especially at the anterior and posterior poles of the epithelium (Fig. 4F,G).

Vps60 controls stalk length and follicle cell organisation in the germarium

To test whether our *in vivo* RNAi screen provides a basis to gain new insights into the mechanisms controlling epithelial development, we selected one gene to characterise further as a proof of principle for our approach. We aimed first to validate the RNAi phenotype of a so far uncharacterised gene, and second to elucidate how this gene controls epithelial development. We chose the gene *CG6259* because it encodes a protein with a clearly predictable function and because it has an advantageous genomic localisation that allows the site-specific generation of null mutants using nearby inserted transposons. Moreover, its knockdown results in a phenotype that is only rudimentarily understood: the formation of elongated stalks.

CG6259 is the fly orthologue of yeast *Vps60* (Kranz et al., 2001) and mammalian *CHMP5* (Shim et al., 2006), which are members of the *Vps4* complex. This complex cooperates with the ESCRT complexes in diverse cellular processes. A pivotal role of the *Vps4* and ESCRT complexes is the generation of multivesicular bodies (MVBs) during endosomal sorting. *Vps60* acts in a late step of vesicle formation by supporting the dissociation of the ESCRT complex from invaginating membranes (for review, see Babst, 2011; Henne et al., 2011).

Closer inspection of the *CG6259/Vps60* RNAi phenotype revealed that not only the stalk length but also the arrangement of germline cysts in the germarium was affected. In wild-type germaria, individual cysts normally string together in a well-arranged manner in region 2 and 3 (Fig. 5A, dashed lines), *Vps60* RNAi disturbs proper cyst alignment (Fig. 5C).

To validate the RNAi phenotype of *Drosophila Vps60*, we generated a null mutation with the help of two piggy back transposons flanking the gene (see Materials and Methods). As homozygous *Vps60* mutants are lethal, we generated genetic mosaics using the FLP/FRT method (Xu and Rubin, 1993). Germaria that consist mostly of *Vps60* mutant cells showed misalignment of cysts and elongated stalks (Fig. 6A). Thus, *Vps60*-null mutants displayed the same phenotype as in the RNAi knockdown validating our screening approach.

A role for the ESCRT complex in controlling germarium and stalk organisation

Knockdown of ESCRT members included in our screen showed a similar phenotype to that of *Vps60*. Knockdown of *Vps20* (ESCRT-III), *Vps25* (ESCRT-II) and *Vps28* (ESCRT-I) result in the same disorganisation of germaria like *Vps60* (Fig. 5E,G; data not shown). Moreover, their knockdown leads to an increase in the number of cells connecting follicles at later stages of oogenesis (Fig. 5F,H). In contrast to *Vps60* RNAi however, where these cells formed a clearly distinguishable stalk (Fig. 5D), *Vps20* and *Vps25* RNAi cells neither adopted the typical disc-shape nor aligned in well-organised cell rows. Consistent with previous reports, we found that at later stages of oogenesis some of these cells accumulated at the poles of egg chambers (Fig. 5F,H, arrowheads) (Vaccari and Bilder, 2005). Thus *Vps20*, *Vps25* and *Vps28* not only restrict the number of cells between two egg chambers but also affect their ability to form a proper stalk.

It has been shown that mutants in the ESCRT-I and ESCRT-II complexes produce a stronger phenotype than mutants in the ESCRT-III complex indicating that loss of early acting ESCRT

components affects tissue architecture more strongly than loss of late acting components (Vaccari et al., 2009). The stronger phenotype of *Vps20*, *Vps25* and *Vps28* (compared to *Vps60*) therefore most likely reflects their roles in earlier steps of MVB biogenesis. Despite their different phenotypic strengths *Vps20*, *Vps25*, *Vps28* and *Vps60* are all required for germarial organisation and to restrict the number of cells connecting two follicles. This supports the idea that they cooperate in the germarium as a part of the ESCRT machinery.

To validate this role of the ESCRT machinery with mutants we chose members of the ESCRT-II (*Vps25*) and ESCRT-I complex (*TSG101/erupted/Vps23*). Analysis of genetic mosaics revealed cyst misalignment (Fig. 6B,C), as well as increased cell numbers between egg chambers, validating the RNAi phenotypes (Fig. 6D,E).

The ESCRT machinery restricts follicle cell proliferation specifically in the germarium

ESCRT proteins act as tumour suppressors and are known to restrict epithelial proliferation in imaginal discs (Moberg et al., 2005; Thompson et al., 2005; Vaccari and Bilder, 2005; Herz et al., 2006). This raises the possibility that the above-described phenotypes are caused by overproliferation. Consistently, elongated stalks have been reported to form after overproliferation of follicle stem cells (Forbes et al., 1996; Zhang and Kalderon, 2000; Zhang and Kalderon, 2001; Song and Xie, 2003). To analyse cell proliferation after knockdown of ESCRT components, we stained ovaries with an antibody against phospho-Histone H3, and found a fourfold increase in dividing epithelial cells (Fig. 7E). Strikingly, overproliferation was exclusively detected in germaria, whereas no increase was detected in mature stalk cells or in egg chambers outside of the germarium (Fig. 7E). Thus, the ESCRT machinery controls mitosis specifically in the germarium, suggesting that there is a spatially restricted ESCRT function in the control of proliferation.

To better define where within the germarium the ESCRT machinery controls proliferation we used Fasciclin3 (*Fas3*) as a landmark, which allows the subdivision of germaria into regions with low and high *Fas3* expression (Fig. 7A) (Zhang and Kalderon, 2001; Nystul and Spradling, 2010). The low-*Fas3* region includes follicle stem cells and their migrating daughters, while in the more posteriorly located high-*Fas3* domain follicle cells start to polarise and undergo MET. After knockdown of ESCRT components we found additional mitoses in both *Fas3* domains (Fig. 7E). Most of the extra divisions, however, occurred in the high-*Fas3* domain, where the average number of mitoses increased from two to seven or eight (Fig. 7B,E). Thus, the ESCRT machinery acts also outside of the stem cell region to restrict epithelial proliferation.

The ESCRT machinery downregulates Notch and JAK/STAT function in the germarium

The majority of the extra cell divisions that occurred after knockdown of ESCRT components took place outside of the stem cell region suggesting that these divisions are the major cause for the disorganisation of germaria and for the formation of elongated stalks. This raises the question of how cell proliferation is controlled outside of the stem cell region. A possible answer is suggested by data from ESCRT mutant cells in *Drosophila* imaginal discs, where the endosomal activation of Notch leads to the production of the JAK/STAT ligand Unpaired, which induces overproliferation (Moberg et al., 2005; Vaccari and Bilder, 2005; Herz et al., 2006). Thus, increased Notch and JAK/

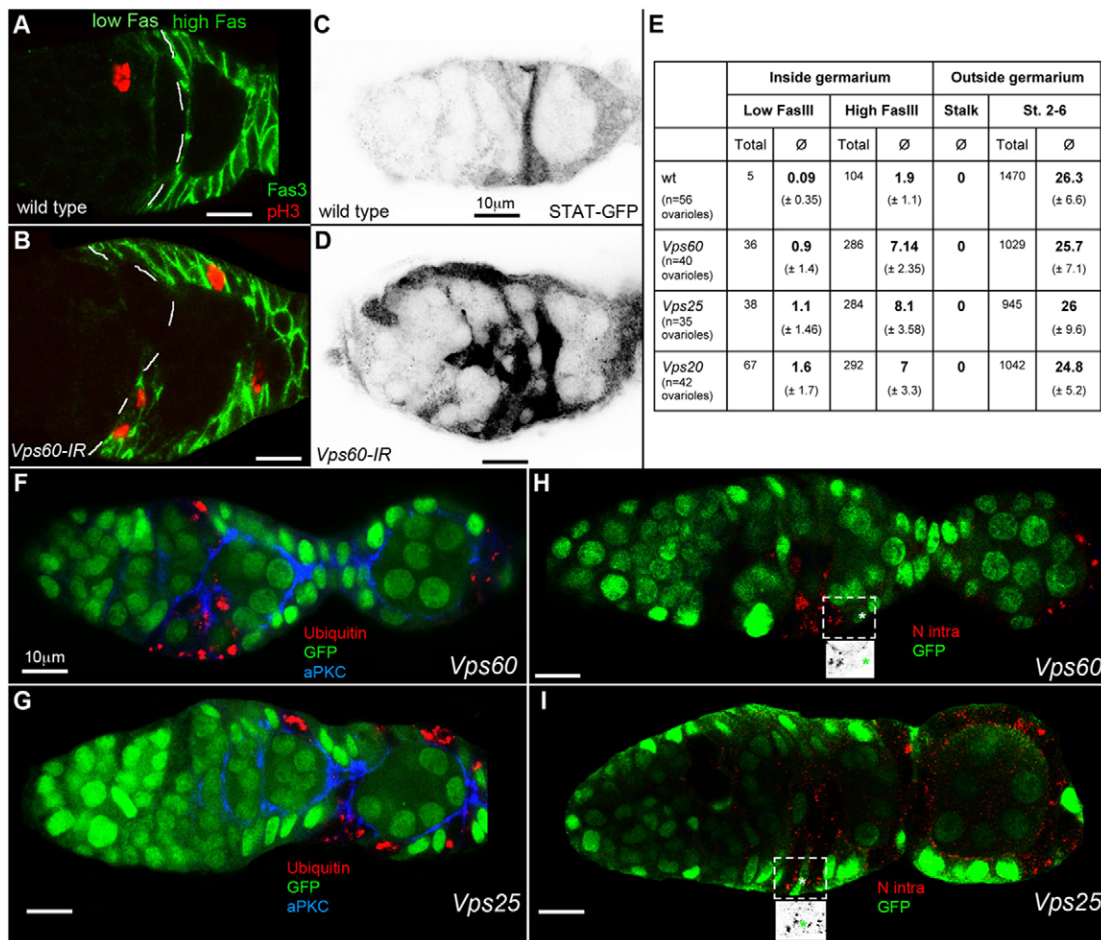


Fig. 7. Depletion of *Vps60* and *Vps25* results in Ubiquitin and N intra accumulation, cell division increase and upregulation of JAK/STAT activity. (A,B) Analysis of cell division. Wild-type (A) and *Vps60*-depleted (B) egg chambers stained for phosphor-Histone 3 (red), revealing cells in mitosis, and for Fas3 (green) subdividing the germarium into a low- and high-Fas3 domain. Only one mitosis is visible in the wild-type germarium, whereas four mitoses are detected in the *Vps60*-depleted germarium. (C,D) Analysis of a JAK/STAT GFP reporter. In the wild-type germarium (C) only one elongated cell shows strong JAK/STAT activity, while almost all follicle cells show high GFP expression after *Vps60* RNAi (D). (E) Counts of cells with phospho-Histone H3 expression, marking cells in mitosis. Regions where cell divisions occur are distinguished into four different regions: the low- and high-Fas3 domains within the germarium, the stalk and stage 2 to stage 6 egg chambers (st. 2–6). (F–I) Analysis of genetic mosaics. Mutant cell clones are marked by the absence of GFP (green). Germaria with small cell clones mutant for *Vps60* (F) and *Vps25* (G) stained for Ubiquitin (red) and aPKC (blue). Germaria with small clones mutant for *Vps60* (H) and *Vps25* (I) stained with an antibody against the intracellular domain of Notch (N intra, red). Insets show N intra channel alone with a wild-type cell marked by an asterisk.

STAT functions could be responsible for increased follicle cell proliferation outside of the stem cell niche. This idea is supported by previous studies showing that overactivation of both pathways results in the formation of elongated stalks. Activation of Notch and loss of Hairless (a negative regulator of Notch signalling) within the germarium produce elongated stalks (Larkin et al., 1996; López-Schier and St Johnston, 2001). Similarly, overexpression of Unpaired results in elongated stalks (McGregor et al., 2002).

To test whether *Vps60* regulates JAK/STAT activity we quantified the expression of a GFP reporter (Bach et al., 2007) in wild-type and *Vps60*-knockout germaria by counting cells with high reporter activity in germarial region 2a and 2b. *Vps60* RNAi leads to a tenfold increase of cells with high JAK/STAT activity (0.9 ± 1.16 cells in wild-type and 10 ± 4.65 cells after *Vps60* RNAi) indicating an important function of *Vps60* in downregulating the pathway in the germarium (Fig. 7C,D). We also analysed reporter activity after *Vps20* and *Vps25* RNAi and

detected a dramatic increase indicating that JAK/STAT activity in the germarium is restricted by the ESCRT machinery (data not shown).

To examine whether the ESCRT machinery affects the Notch pathway in the germarium, we stained ovaries of genetic mosaics with an antibody detecting the cytoplasmic domain of Notch (N intra). Although N intra is only faintly detectable in wild-type cells, *Vps60* and *Vps25* mutant cells strongly accumulated the protein in the cytoplasm (Fig. 7H,I). The accumulation of N intra in ESCRT mutant cells in the germarium suggests that the endocytosed Notch protein cannot be degraded properly, which could result in increased Notch function.

To test whether the defects in ESCRT mutants are caused by increased Notch function we knocked down *Notch* in ovarioles with *Vps60* mutant cell clones and performed double RNAi experiments. Control ovaries with *Notch* knockdown and normal ESCRT function resulted in the absence of stalks (supplementary

material Fig. S2C). This phenotype was previously reported for *Notch* mutants (Ruohola et al., 1991; López-Schier and St Johnston, 2001). Ovarioles with *Notch* and *Vps60* double RNAi as well as ovarioles that mainly consist of *Vps60* mutant cells, in which Notch is depleted, showed a normal arrangement of cysts in the germarium and did not form stalks (supplementary material Fig. S2B,D). This indicates that the formation of elongated stalks and the disorganisation of germaria in ESCRT mutants are dependent on *Notch* function.

Increased follicle cell proliferation in ESCRT depleted germaria is Notch dependent

A major function of the ESCRT machinery is the formation of MVBs in which endocytosed signalling receptors are inactivated. This process is crucial for the downregulation of multiple signalling pathways during development (Rusten et al., 2011). A hallmark of impaired ESCRT function is the cytoplasmic accumulation of ubiquitylated proteins, which are targeted for degradation but fail to be internalised into MVBs. To test whether MVB formation is affected in follicle cell precursors mutant for *Vps60* and *Vps25* we stained mosaic ovaries for Ubiquitin. Both mutants showed a dramatic Ubiquitin accumulation in the cytoplasm of follicle cells indicating strong defects in the endolysosomal pathway (Fig. 7F,G).

We tested whether increased Notch function contributes to Ubiquitin accumulation in ESCRT mutant cells. Notably, *Vps60* mutant cells in which Notch is depleted show a strong reduction in the cytoplasmic accumulation of Ubiquitin (supplementary material Fig. S2B). This suggests that a major reason for Ubiquitin accumulation in ESCRT mutant cells is increased *Notch* function. The cytoplasmic aggregation of Ubiquitin in ESCRT mutant cells could reflect the accumulation of N intra itself, and additionally of components of other signalling pathways that are downstream of Notch (e.g. JAK/STAT). The finding that the strong reduction of the cytoplasmic Ubiquitin accumulation is accompanied by a suppression of the morphological defects of *Vps60* mutants is consistent with the idea that the defects in germarial organisation and stalk formation are caused by a failure in MVB formation and protein degradation.

To directly address the question whether increased proliferation rates in ESCRT-depleted germaria are caused by increased Notch function we analysed double-knockdown experiments. Control experiments with *Notch* single RNAi lead to a decrease in follicle cell division in the germarium supporting a positive role of the Notch pathway in proliferation (supplementary material Table S4). Importantly, simultaneous knockdown of *Notch* and ESCRT components results in cell division rates that are similar to those with the *Notch* single RNAi. Thus, increased proliferation rates in ESCRT-depleted germaria are dependent on *Notch*. We therefore conclude that one major mechanism by which the ESCRT complex inhibits cell proliferation in the germarium is downregulation of Notch function.

In summary, our data show that impaired ESCRT function results in intracellular Notch accumulation, increased JAK/STAT activity and increased follicle cell proliferation. Moreover, they indicate that increased cell proliferation in ESCRT-depleted germaria is Notch dependent. As activation of Notch and JAK/STAT pathways are able to induce cell divisions they may directly contribute to increased proliferation in the germarium. Importantly, our data indicate Notch accumulation and increased JAK/STAT signalling in that part of the germarium, where most

of the extra cell divisions occur, and where the mechanisms controlling proliferation are unknown (i.e. the region outside of the stem cell niche).

DISCUSSION

A model explaining the formation of disorganised germaria and elongated stalks

How does increased proliferation in the germarium lead to disorganised germaria and eventually to the formation of elongated stalks? Our data indicate that impaired function of the ESCRT machinery prevents the formation of MVBs and results in the accumulation of signalling proteins in the endolysosomal pathway. We propose that sustained signalling activities cause increased proliferation rates, which affects proper cyst alignment.

The linear alignment of cysts in the germarium is most likely mediated by follicle cells, which are good candidates to influence shape and positioning of cysts. Uncontrolled follicle cell divisions might interfere with normal follicle cell morphology and movements, and thereby disturb proper cyst positioning. Our data indicate increased Notch and JAK/STAT functions in follicle cells, and thus identify these pathways as candidates to induce extra cell divisions.

Notch and JAK/STAT signalling is also required for cell type specification of polar and stalk cells, raising the question as to whether *Vps60* is implicated in this process too. Notch signalling specifies polar cells, which in turn induce stalk cell fate through the JAK/STAT pathway. Recent studies provide evidence that these processes start at the border of the region between 2b and 3 of the germarium (Fig. 1; Nystul and Spradling, 2010; Chang et al., 2013). Our data indicate, however, a strong upregulation of the two pathways already in region 2a and 2b (Fig. 7D,H,I), suggesting that the ESCRT complex already controls Notch and JAK/STAT activity before cell type specification occurs. In support of this view, we see no precocious specification of polar and stalk cells in *Vps60* mutants (supplementary material Fig. S3). The downregulation of Eyes absent (*Eya*) is the earliest marker for the onset of polar/stalk cell specification (Bai and Montell, 2002). Consequently, a precocious polar/stalk cell specification would be accompanied by a premature downregulation of *Eya* in the region between 2b and 3. However, *Vps60* mutant cells show normal *Eya* expression in this region, indicating that the timing of cell specification is not altered.

Notch signalling has an additional earlier function in directing the migration of stem cell daughters between the germline cysts in region 2a and 2b (Nystul and Spradling, 2010). It is possible that Notch overactivation in *Vps60*-deficient stem cell daughters interferes with this process. Thus, disturbed migration, as well as overproliferation, might contribute to the disorganisation in germaria.

Given the defective architecture of *Vps60*-depleted germaria, it is surprising that they produce egg chambers with an apparently normal epithelium. An explanation is provided by the very mild polarity defects of *Vps60* mutant cells, which form adherens junctions and polarised membrane domains (Fig. 6A, insets). Essentially normal polarisation allows the assembly of a monolayered epithelium when egg chambers exit the germarium (Fig. 5D). Owing to increased proliferation rates within the germarium, however, supernumerary cells are produced that are unable to integrate all into this monolayer when the egg chamber buds off. We propose that cells that do not contact to the cyst

accumulate between two follicles and adopt stalk cell fate. Thus, the elongated stalks in *Vps60* mutants reflect supernumerary cells produced by extra cell divisions in the germarium.

Different proliferation domains in the developing follicular epithelium

By characterising the function of *Vps60*, we also identified an unexpected switch in proliferation control during epithelial development. Our data show that *Vps60* and the ESCRT complex control cell division only within the germarium but not in later stages of oogenesis. This indicates that there are ESCRT-dependent proliferation mechanisms within, and ESCRT-independent mechanisms outside of, the germarium, and thus suggests the existence of spatially restricted proliferation domains.

These domains are also reflected by a differential impact of Notch activation on follicle cell proliferation. Notch activation within the germarium leads to elongated stalks (Larkin et al., 1996; López-Schier and St Johnston, 2001), which are most probably generated by extra cell divisions. By contrast, outside of the germarium, Notch activation produces no signs of overproliferation (which would be revealed by multilayering). Consistent with this, normally occurring Notch activation during mid-oogenesis (stage 6) does not induce, but rather prevents, epithelial proliferation (Deng et al., 2001; López-Schier and St Johnston, 2001; Poulton et al., 2011). Thus, it appears that by exiting the germarium egg chambers acquire a new proliferation mode, which is independent of the ESCRT machinery and in which Notch activation is unable to induce mitosis.

Currently it is unknown what determines the switch between the ESCRT-dependent and -independent proliferation modes. The timing of the switch, which coincides with the exit from the germarium, raises the question as to whether the germarium represents a microenvironment with signalling cues that promote Notch-dependent cell proliferation. After budding of the follicle, the epithelium might enter a new microenvironment and acquire a new proliferation mode, which is Notch and ESCRT independent.

In addition to the above-described two proliferation modes, the follicle stem cell niche defines a third region with a specific proliferation mode. During epithelial development each cell encounters these three domains (or microenvironments), in which different modes of proliferation control operate. Cells leave the stem cell niche (domain 1), pass through the remaining germarium (domain 2) and enter the region outside of the germarium (domain 3). As the potential of cells to differentiate (into polar cells, stalk cells and epithelial cells) restricts during oogenesis it is tempting to correlate these domains with a regression of ‘stemness’ over time.

In contrast to the stem cell niche, for which several secreted factors controlling cell division have been identified, the other two proliferation domains are poorly characterised. The genes identified in our *in vivo* RNAi screen provide a valuable source to better characterise the mechanisms controlling proliferation in these domains. Moreover, newly identified genes might help us to discern how the domains are defined. These studies will shed light on the principles of proliferation control in developing epithelial tissues, and will help us to understand misregulation of epithelial proliferation in disease processes.

MATERIALS AND METHODS

Genome-scale RNAi screen

We tested different *in vivo* RNAi conditions in the follicular epithelium in a pilot screen, which included polarity genes with known phenotypes.

This revealed optimal screening conditions when UAS-Dicer2 is coexpressed with the UAS-hairpin (Dietzl et al., 2007) and when crosses are raised at 27°C.

For the primary screen we crossed UAS-hairpin males from the KK library (provided by the VDRC) with females harbouring *escargot*-Gal4 (Micchelli and Perrimon, 2006) and *GRI*-GAL4 (Gupta and Schüpbach, 2003) drivers. A UAS-GFP transgene was coexpressed with the hairpin to visualise the cytoplasm of the epithelial cells. Vials were flipped after 4 days to generate a copy. The first vial was raised continuously at 27°C, whereas the second was raised at 18°C (a temperature at which the UAS/GAL4 system is less active) and shifted to 27°C at pupal stages. If the vial at 27°C produced viable knockout females, these were analysed. If knockout females were lethal (most likely due to gene knockdown at earlier stages of development), flies from the shifted vial were analysed. Crosses that were lethal under both conditions were re-crossed with the *GRI*-GAL4 driver alone. A small proportion of UAS-hairpin constructs was still lethal under these conditions. These were subsequently screened with *traffic jam*-GAL4 (Olivieri et al., 2010), and 12 were still lethal under these conditions.

To generate histological samples of the ovaries in a high-throughput format, we developed a staining method that is based on the use of multiwell filterplates as previously described (Berns et al., 2012). Briefly, ovaries were directly dissected into wells filled with Schneider’s medium, fixed for 10 min with 8% formaldehyde in phosphate-buffered saline (PBS), washed with PBS with 0.1% Tween and subsequently incubated in DAPI (1:1000 dilution of a 1 mg/ml stock). Medium was aspirated by applying vacuum. Filters with ovaries were pushed out and mounted in Vectashield (Vector labs) on a microscope slide. Defects in follicular epithelium were assessed under a fluorescence wide-field microscope by analysing the organisation of the DAPI-stained nuclei and the GFP-labelled epithelial cytoplasm.

Genes whose knockdowns resulted in epithelial defects were further characterised in a classification screen, in which the corresponding KK lines were crossed with *traffic jam*-Gal4. Ovaries of offspring females were dissected in glass dishes and transferred to multiwell filterplates, in which antibody stainings were performed as described previously (Berns et al., 2012). Ovaries were fixed and stained with primary antibodies against aPKC and Dlg, and fluorescently labelled secondary antibodies. Nuclei were stained with DAPI. After staining, ovaries were mounted in Vectashield for microscopic analysis with a wide-field microscope. Defects were classified according to the different phenotypic groups (see Table 1) and the overall penetrance of epithelial defects was evaluated. We subdivided the penetrance into three main groups: strong penetrance (100–75% of the ovarioles were affected), medium penetrance (75–50%) and weak penetrance (50–25%).

Gene Ontology (GO) term enrichment analysis

All genes in one phenotypic category were analysed for an enrichment of GO terms describing cellular processes using the tool ‘term enrichment’ in the AmiGO (version 1.8) web application (<http://amigo.geneontology.org>) (Carbon et al., 2009). A list of all screened KK lines was used as the background set and filtered with Fly Base database. ‘Inferred from electronic annotation’ (IEA) was used and a maximum *P*-value of 0.01 selected. As GO terms at a deeper level in the tree hierarchy are considered to be more biologically informative, we discarded terms containing more than 500 genes from further analysis according to the example of Neely et al. (Neely et al., 2010). For Table 1, significant terms were manually curated for its relevance with reference to the observed phenotype. A complete list of enriched GO terms in the different phenotypic categories is provided in supplementary material Table S2.

Antibodies, histology and microscopy

Antibodies used in this study were as follows: rabbit anti-phospho-Histone H3 1:500 (Upstate, Millipore), mouse anti-Eyes absent [1:25; Developmental Studies Hybridoma Bank (DSHB), clone *eya10H6*], mouse anti-Armadillo (1:200; DSHB, clone N2 7A1), rabbit anti-aPKC (1:100; Santa Cruz Biotechnology, sc-216), mouse anti-Discs Large (1:50; DSHB, clone 4F3), mouse anti-Fasciclin 3 (1:200; DSHB, clone

7G10), mouse anti-Notch intracellular domain (1:50; DSHB, C17.9C6), rabbit anti-GFP (1:200; Invitrogen) and goat anti-GFP-FITC (1:100; GeneTex, GTX26662), mouse anti-mono- and polyubiquitinated conjugates (1:100; FK2, Enzo Lifescience, BML-PW8810). Alexa-Fluor-coupled (Alexa Fluor 488, 568 and 647) secondary antibodies (Invitrogen) were used in a 1:400 dilution.

Images were acquired using a Leica SP5 or Carl Zeiss LSM-700 confocal microscope at room temperature (20–22°C). All pictures were acquired with a 40× oil immersion magnification. For the Carl Zeiss LSM-700 microscope, the 40× objective numerical aperture (NA) is 1.3; for Leica SP5 microscope, the 40× objective NA is 1.25. The pictures were edited and the figures were assembled with Adobe Photoshop CS3. Processing of the images involved adjustment of gamma settings.

Generation of *Vps60* mutants

To generate a deletion uncovering the *CG6259* (*Vps60*) locus, we used two transposons carrying FRT sites, which allowed the recovery of chromosomes with deletions of molecularly defined end points (Parks et al., 2004). Following the instructions of Parks et al., chromosomes harbouring the transposons d08528 and f02548 (provided by the Exelixis collection at the Harvard Medical School) were crossed in trans to induce a small deficiency that we named Df(3L)d08528-f02548 and which uncovers the entire open reading frame of *Vps60* but of no other gene. The deletion was recombined with FRT2A to generate genetic mosaic flies as described below.

Generation of genetic mosaics

Flies carrying the mutant allele on a chromosome with a FRT site were crossed to males carrying the respective wild-type allele, a GFP reporter gene and a FRT site. Crosses were raised at 27°C. Mitotic cell clones were induced with a FLP recombinase under the control of a heat-shock promoter located on a different chromosome (Xu and Rubin, 1993). Heat shocks for clone induction were performed by placing vials, for 1 hour, in a 37°C water bath. For *Tsg101* and *Vps25*, several heat shocks were provided during larval stages. Newly hatched flies were raised at 27°C and dissected the next day. To generate small *Vps25* mutant clones in the gerarium, newly hatched females were heat shocked on 2 days, raised for one more day at 27°C and dissected. Clones for *Vps60* were generated by raising flies at 27°C and providing two heat shocks in late pupal stages (day 8 and 9). After clone induction, adult females were raised for 2–3 days at 18°C. Ovaries with *Vps60* clones with simultaneous Notch RNAi were generated by inducing UAS-N-IR (KK line) with *traffic jam*-GAL4. Females were raised at 18°C until pupal stages and shifted to 21°C. Several heat shocks were provided during larval stages. Ovaries were dissected as described previously (Franz and Riechmann, 2010).

Fly strains

Fly strains used were as follows: (1) w UAS-*Dicer2*; *escargot*-GAL4 (Micchelli and Perrimon, 2006) UAS-GFP/CyO; *GRI*-GAL4 (Gupta and Schüpbach, 2003)/TM3 Sb; (2) w UAS-*Dicer2*; *traffic jam*-GAL4 (Olivieri et al., 2010); (3) w ;;Df(3L)d08528-f02548 FRT2A/TM6 Sb (this study); (4) w;; *ept-1²* FRT80B/TM6b (mutant allele of *TSG101*, (Moberg et al., 2005); (5) w; *Vps25⁴³* FRT42D/CyO (Vaccari and Bilder, 2005); and (6) w UAS-*Dicer2*; *traffic jam*-GAL4 10XSTAT92E-GFP (Bach et al., 2007)/CyO.

Quantification of cell proliferation and JAK/STAT activity

Knockdown of components of the ESCRT machinery were induced with *traffic jam*-GAL4. Crosses for *Vps60* RNAi were raised continuously at 27°C. As *Vps20*, *Vps25* and *Vps28* knockdowns generate, to a large extent, very small ovaries under these conditions, we raised these crosses at 18°C until late pupal stages and then shifted the vials to 27°C for 2–3 days. This resulted in ovaries of approximately normal volumes.

To quantify the number of cells in mitosis, ovaries were stained with antibodies against phospho-Histone H3 and Fas3. Mitosis events were counted under a wide-field microscope and allocated either to the low-Fas3 or high-Fas3 domain within the gerarium or to the region outside

of the gerarium. Defects in stalk morphology in *Vps20* and *Vps25* knockdown ovaries made it difficult for some ovaries to distinguish the gerarium from later oogenesis stages. In these cases we analysed the anterior high Fas3 region comprising up to 5–6 cysts.

To quantify cells with high JAK/STAT activity, confocal pictures of optical mid-sagittal sections of geraria stained for Fas3, GFP and DAPI were analysed. All pictures were taken with the same confocal setup, which was adjusted for the intensity of the JAK/STAT-GFP signal in *Vps60*-knockdown geraria. Regions expressing strong levels of GFP were counted and assigned to individual cells with the help of DAPI-stained nuclei. See Fig. 7G,H for examples which show the JAK/STAT channel alone.

Acknowledgements

We thank Siegfried Roth (Cologne University, Germany) and Muriel Grammont (Lyon University, France) for helpful comments on the manuscript, the VDRC, the TRiP at Harvard Medical School (NIH/NIGMS R01-GM084947), Bloomington stock centre, and Thomas Vaccari (IFOM - FIRC Institute of Molecular Oncology, Milan, Italy), Jerome Korzelius (Heidelberg University, Germany) and Bruce Edgar (Heidelberg University, Germany) for providing fly stocks and DSHB for providing antibodies. We acknowledge the support of the Core Facility Life Cell Imaging Mannheim at the CBTM (DFG INST 91027/9-1 FUGG) and the German Cancer Research Center Light Microscopy Facility.

Competing interests

The authors declare no competing interests.

Author contributions

The screen was performed by N.B., I.W. and N.K. S.F. generated the *Vps60* mutants. The phenotype of the ESCRT components was analysed by N.B. and S.F. V.R. designed the concept of the screen and prepared the manuscript.

Funding

The project was funded by grants from the Deutsche Krebshilfe (project 110208); from the Deutsche Forschungsgemeinschaft (Sachmittelbeihilfe and SFB 572); and by the EU FP7 Project CancerPathways.

Supplementary material

Supplementary material available online at <http://jcs.biologists.org/lookup/suppl/doi:10.1242/jcs.144519/-DC1>

References

- Assa-Kunik, E., Torres, I. L., Schejter, E. D., Johnston, D. S. and Shilo, B. Z. (2007). Drosophila follicle cells are patterned by multiple levels of Notch signaling and antagonism between the Notch and JAK/STAT pathways. *Development* **134**, 1161–1169.
- Babst, M. (2011). MVB vesicle formation: ESCRT-dependent, ESCRT-independent and everything in between. *Curr. Opin. Cell Biol.* **23**, 452–457.
- Bach, E. A., Ekas, L. A., Ayala-Camargo, A., Flaherty, M. S., Lee, H., Perrimon, N. and Baeg, G. H. (2007). GFP reporters detect the activation of the Drosophila JAK/STAT pathway in vivo. *Gene Expr. Patterns* **7**, 323–331.
- Bai, J. and Montell, D. (2002). Eyes absent, a key repressor of polar cell fate during Drosophila oogenesis. *Development* **129**, 5377–5388.
- Baksa, K., Parke, T., Dobens, L. L. and Dearolf, C. R. (2002). The Drosophila STAT protein, stat92E, regulates follicle cell differentiation during oogenesis. *Dev. Biol.* **243**, 166–175.
- Berns, N., Woichansky, I., Kraft, N., Hüsken, U., Carl, M. and Riechmann, V. (2012). "Vacuum-assisted staining": a simple and efficient method for screening in Drosophila. *Dev. Genes Evol.* **222**, 113–118.
- Bilder, D. (2004). Epithelial polarity and proliferation control: links from the Drosophila neoplastic tumor suppressors. *Genes Dev.* **18**, 1909–1925.
- Bilder, D., Li, M. and Perrimon, N. (2000). Cooperative regulation of cell polarity and growth by Drosophila tumor suppressors. *Science* **289**, 113–116.
- Carbon, S., Ireland, A., Mungall, C. J., Shu, S., Marshall, B., Lewis, S.; AmiGO Hub; Web Presence Working Group (2009). AmiGO: online access to ontology and annotation data. *Bioinformatics* **25**, 288–289.
- Chang, Y. C., Jang, A. C., Lin, C. H. and Montell, D. J. (2013). Castor is required for Hedgehog-dependent cell-fate specification and follicle stem cell maintenance in Drosophila oogenesis. *Proc. Natl. Acad. Sci. USA* **110**, E1734–E1742.
- Deng, W. M., Althausen, C. and Ruohola-Baker, H. (2001). Notch-Delta signaling induces a transition from mitotic cell cycle to endocycle in Drosophila follicle cells. *Development* **128**, 4737–4746.
- Dietz, G., Chen, D., Schnorrer, F., Su, K. C., Barinova, Y., Fellner, M., Gasser, B., Kinsey, K., Oppel, S., Scheiblaue, S. et al. (2007). A genome-wide transgenic RNAi library for conditional gene inactivation in Drosophila. *Nature* **448**, 151–156.

- Forbes, A. J., Lin, H., Ingham, P. W. and Spradling, A. C. (1996). hedgehog is required for the proliferation and specification of ovarian somatic cells prior to egg chamber formation in *Drosophila*. *Development* **122**, 1125–1135.
- Franz, A. and Riechmann, V. (2010). Stepwise polarisation of the *Drosophila* follicular epithelium. *Dev. Biol.* **338**, 136–147.
- Georgiou, M., Marinari, E., Burden, J. and Baum, B. (2008). Cdc42, Par6, and aPKC regulate Arp2/3-mediated endocytosis to control local adherens junction stability. *Curr. Biol.* **18**, 1631–1638.
- Grammont, M. and Irvine, K. D. (2001). fringe and Notch specify polar cell fate during *Drosophila* oogenesis. *Development* **128**, 2243–2253.
- Gupta, T. and Schüpbach, T. (2003). Cct1, a phosphatidylcholine biosynthesis enzyme, is required for *Drosophila* oogenesis and ovarian morphogenesis. *Development* **130**, 6075–6087.
- Harris, K. P. and Tepass, U. (2008). Cdc42 and Par proteins stabilize dynamic adherens junctions in the *Drosophila* neuroectoderm through regulation of apical endocytosis. *J. Cell Biol.* **183**, 1129–1143.
- Henne, W. M., Buchkovich, N. J. and Emr, S. D. (2011). The ESCRT pathway. *Dev. Cell* **21**, 77–91.
- Herz, H. M., Chen, Z., Scherr, H., Lackey, M., Bolduc, C. and Bergmann, A. (2006). vps25 mosaics display non-autonomous cell survival and overgrowth, and autonomous apoptosis. *Development* **133**, 1871–1880.
- Horne-Badovinac, S. and Bilder, D. (2005). Mass transit: epithelial morphogenesis in the *Drosophila* egg chamber. *Dev. Dyn.* **232**, 559–574.
- Joberty, G., Petersen, C., Gao, L. and Macara, I. G. (2000). The cell-polarity protein Par6 links Par3 and atypical protein kinase C to Cdc42. *Nat. Cell Biol.* **2**, 531–539.
- Kirilly, D., Spana, E. P., Perrimon, N., Padgett, R. W. and Xie, T. (2005). BMP signaling is required for controlling somatic stem cell self-renewal in the *Drosophila* ovary. *Dev. Cell* **9**, 651–662.
- Kranz, A., Kinner, A. and Kölling, R. (2001). A family of small coiled-coil-forming proteins functioning at the late endosome in yeast. *Mol. Biol. Cell* **12**, 711–723.
- LaFever, L. and Drummond-Barbosa, D. (2005). Direct control of germline stem cell division and cyst growth by neural insulin in *Drosophila*. *Science* **309**, 1071–1073.
- Larkin, M. K., Holder, K., Yost, C., Giniger, E. and Ruohola-Baker, H. (1996). Expression of constitutively active Notch arrests follicle cells at a precursor stage during *Drosophila* oogenesis and disrupts the anterior-posterior axis of the oocyte. *Development* **122**, 3639–3650.
- Leibfried, A., Fricke, R., Morgan, M. J., Bogdan, S. and Bellaiche, Y. (2008). *Drosophila* Cip4 and WASp define a branch of the Cdc42-Par6-aPKC pathway regulating E-cadherin endocytosis. *Curr. Biol.* **18**, 1639–1648.
- Lin, D., Edwards, A. S., Fawcett, J. P., Mbamalu, G., Scott, J. D. and Pawson, T. (2000). A mammalian PAR-3-PAR-6 complex implicated in Cdc42/Rac1 and aPKC signalling and cell polarity. *Nat. Cell Biol.* **2**, 540–547.
- López-Schier, H. and St Johnston, D. (2001). Delta signaling from the germ line controls the proliferation and differentiation of the somatic follicle cells during *Drosophila* oogenesis. *Genes Dev.* **15**, 1393–1405.
- Lu, H. and Bilder, D. (2005). Endocytic control of epithelial polarity and proliferation in *Drosophila*. *Nat. Cell Biol.* **7**, 1232–1239.
- McGregor, J. R., Xi, R. and Harrison, D. A. (2002). JAK signaling is somatically required for follicle cell differentiation in *Drosophila*. *Development* **129**, 705–717.
- Micchelli, C. A. and Perrimon, N. (2006). Evidence that stem cells reside in the adult *Drosophila* midgut epithelium. *Nature* **439**, 475–479.
- Moberg, K. H., Schelble, S., Burdick, S. K. and Hariharan, I. K. (2005). Mutations in erupted, the *Drosophila* ortholog of mammalian tumor susceptibility gene 101, elicit non-cell-autonomous overgrowth. *Dev. Cell* **9**, 699–710.
- Morrison, H. A., Dionne, H., Rusten, T. E., Brech, A., Fisher, W. W., Pfeiffer, B. D., Celniker, S. E., Stenmark, H. and Bilder, D. (2008). Regulation of early endosomal entry by the *Drosophila* tumor suppressors Rabenosyn and Vps45. *Mol. Biol. Cell* **19**, 4167–4176.
- Müller, H. A. (2000). Genetic control of epithelial cell polarity: lessons from *Drosophila*. *Dev. Dyn.* **218**, 52–67.
- Neely, G. G., Kuba, K., Cammarato, A., Isobe, K., Amann, S., Zhang, L., Murata, M., Elmén, L., Gupta, V., Arora, S. et al. (2010). A global in vivo *Drosophila* RNAi screen identifies NOT3 as a conserved regulator of heart function. *Cell* **141**, 142–153.
- Nystul, T. and Spradling, A. (2007). An epithelial niche in the *Drosophila* ovary undergoes long-range stem cell replacement. *Cell Stem Cell* **1**, 277–285.
- Nystul, T. and Spradling, A. (2010). Regulation of epithelial stem cell replacement and follicle formation in the *Drosophila* ovary. *Genetics* **184**, 503–515.
- Olivieri, D., Sykora, M. M., Sachidanandam, R., Mechtler, K. and Brennecke, J. (2010). An in vivo RNAi assay identifies major genetic and cellular requirements for primary piRNA biogenesis in *Drosophila*. *EMBO J.* **29**, 3301–3317.
- Parks, A. L., Cook, K. R., Belvin, M., Dompe, N. A., Fawcett, R., Huppert, K., Tan, L. R., Winter, C. G., Bogart, K. P., Deal, J. E. et al. (2004). Systematic generation of high-resolution deletion coverage of the *Drosophila melanogaster* genome. *Nat. Genet.* **36**, 288–292.
- Poulton, J. S., Huang, Y. C., Smith, L., Sun, J., Leake, N., Schleede, J., Stevens, L. M. and Deng, W. M. (2011). The microRNA pathway regulates the temporal pattern of Notch signaling in *Drosophila* follicle cells. *Development* **138**, 1737–1745.
- Qiu, R. G., Abo, A. and Steven Martin, G. (2000). A human homolog of the *C. elegans* polarity determinant Par-6 links Rac and Cdc42 to PKCzeta signaling and cell transformation. *Curr. Biol.* **10**, 697–707.
- Ruohola, H., Bremer, K. A., Baker, D., Swedlow, J. R., Jan, L. Y. and Jan, Y. N. (1991). Role of neurogenic genes in establishment of follicle cell fate and oocyte polarity during oogenesis in *Drosophila*. *Cell* **66**, 433–449.
- Rusten, T. E., Vaccari, T. and Stenmark, H. (2011). Shaping development with ESCRTs. *Nat. Cell Biol.* **14**, 38–45.
- Sarpal, R., Pellikka, M., Patel, R. R., Hui, F. Y., Godt, D. and Tepass, U. (2012). Mutational analysis supports a core role for *Drosophila* α -catenin in adherens junction function. *J. Cell Sci.* **125**, 233–245.
- Schnorrer, F., Kalchauer, I. and Dickson, B. J. (2007). The transmembrane protein Kon-tiki couples to Dgrip to mediate myotube targeting in *Drosophila*. *Dev. Cell* **12**, 751–766.
- Shim, J. H., Xiao, C., Hayden, M. S., Lee, K. Y., Trombetta, E. S., Pypaert, M., Nara, A., Yoshimori, T., Wilm, B., Erdjument-Bromage, H. et al. (2006). CHMP5 is essential for late endosome function and down-regulation of receptor signaling during mouse embryogenesis. *J. Cell Biol.* **172**, 1045–1056.
- Song, X. and Xie, T. (2003). Wingless signaling regulates the maintenance of ovarian somatic stem cells in *Drosophila*. *Development* **130**, 3259–3268.
- Spradling, A. C. (1993). Developmental genetics of oogenesis. In *The Development of Drosophila Melanogaster*, Vol. 1 (ed. M. Bate and A. Martinez-Arias). Cold Spring Harbor, NY: Cold Spring Harbor Laboratory Press.
- Tanentzapf, G., Smith, C., McGlade, J. and Tepass, U. (2000). Apical, lateral, and basal polarization cues contribute to the development of the follicular epithelium during *Drosophila* oogenesis. *J. Cell Biol.* **151**, 891–904.
- Tepass, U., Tanentzapf, G., Ward, R. and Fehon, R. (2001). Epithelial cell polarity and cell junctions in *Drosophila*. *Annu. Rev. Genet.* **35**, 747–784.
- Thompson, B. J., Mathieu, J., Sung, H. H., Loeser, E., Rørth, P. and Cohen, S. M. (2005). Tumor suppressor properties of the ESCRT-II complex component Vps25 in *Drosophila*. *Dev. Cell* **9**, 711–720.
- Torres, I. L., López-Schier, H. and St Johnston, D. (2003). A Notch/Delta-dependent relay mechanism establishes anterior-posterior polarity in *Drosophila*. *Dev. Cell* **5**, 547–558.
- Vaccari, T. and Bilder, D. (2005). The *Drosophila* tumor suppressor vps25 prevents nonautonomous overproliferation by regulating notch trafficking. *Dev. Cell* **9**, 687–698.
- Vaccari, T., Rusten, T. E., Menut, L., Nezis, I. P., Brech, A., Stenmark, H. and Bilder, D. (2009). Comparative analysis of ESCRT-I, ESCRT-II and ESCRT-III function in *Drosophila* by efficient isolation of ESCRT mutants. *J. Cell Sci.* **122**, 2413–2423.
- Verni, F., Somma, M. P., Gunsalus, K. C., Bonaccorsi, S., Belloni, G., Goldberg, M. L. and Gatti, M. (2004). Feo, the *Drosophila* homolog of PRC1, is required for central-spindle formation and cytokinesis. *Curr. Biol.* **14**, 1569–1575.
- Vied, C., Reilein, A., Field, N. S. and Kalderon, D. (2012). Regulation of stem cells by intersecting gradients of long-range niche signals. *Dev. Cell* **23**, 836–848.
- Wang, Y. and Riechmann, V. (2007). The role of the actomyosin cytoskeleton in coordination of tissue growth during *Drosophila* oogenesis. *Curr. Biol.* **17**, 1349–1355.
- Xi, R., McGregor, J. R. and Harrison, D. A. (2003). A gradient of JAK pathway activity patterns the anterior-posterior axis of the follicular epithelium. *Dev. Cell* **4**, 167–177.
- Xu, T. and Rubin, G. M. (1993). Analysis of genetic mosaics in developing and adult *Drosophila* tissues. *Development* **117**, 1223–1237.
- Zhang, Y. and Kalderon, D. (2000). Regulation of cell proliferation and patterning in *Drosophila* oogenesis by Hedgehog signaling. *Development* **127**, 2165–2176.
- Zhang, Y. and Kalderon, D. (2001). Hedgehog acts as a somatic stem cell factor in the *Drosophila* ovary. *Nature* **410**, 599–604.